Submitted to the Astrophysical Journal
Preprint typeset using LaTeX style emulateapj v. 6/22/04



# THE EXPANSION ASYMMETRY AND AGE OF THE CASSIOPEIA A SUPERNOVA REMNANT[1]

Robert A. Fesen[2], Molly C. Hammell[2], Jon Morse[3], Roger A. Chevalier[4], Kazimierz J. Borkowski[5], Michael A. Dopita[6], Christopher L. Gerardy[7], Stephen S. Lawrence[8], John C. Raymond[9], & Sidney van den Bergh[10]

*Submitted to the Astrophysical Journal*

## ABSTRACT

*HST* images of the young supernova remnant Cas A are used to explore the expansion and spatial distribution of its highest velocity debris. ACS/WFC images taken in March and December 2004 with Sloan F625W, F775W, and F850LP filters were used to identify 1825 high-velocity, outlying ejecta knots through measured proper motions of $0\farcs35 - 0\farcs90$ yr$^{-1}$ corresponding to $V_{trans} = 5500 - 14500$ km s$^{-1}$ assuming d = 3.4 kpc. The distribution of derived transverse expansion velocities for these ejecta knots shows a striking bipolar asymmetry with the highest velocity knots ($V_{trans} \geq 10500$ km s$^{-1}$) confined to nearly opposing northeast and southwest 'jets' at P.A. = $45° - 70°$ and $230° - 270°$, respectively. The jets have about the same maximum expansion velocity of $\simeq$14000 km s$^{-1}$ and appear kinematically and chemically distinct in that they are the remnant's only S-rich ejecta with expansion velocities above the $10000 - 11000$ km s$^{-1}$ exhibited by outer nitrogen-rich ejecta which otherwise represent the remnant's highest velocity debris. In addition, we find significant gaps in the spatial distribution of outlying ejecta in directions which are approximately perpendicular to the jets (P.A. = $145° - 200°$ and $335° - 350°$). The remnant's central X-ray point source lies some 7″ to the southeast of the estimated expansion center (PA = $169° \pm 8.4°$) indicating a projected motion toward the middle of the broad southern ejecta knot gap. Extrapolations of measured nine month proper motions for all 1825 outer ejecta knots and a selected subsample of 72 bright and compact knots suggest explosion dates (assuming no knot deceleration) of $1662 \pm 27$ and $1672 \pm 18$, respectively. We find some evidence for non-uniform deceleration in different directions around the remnant and find 126 knots located along the northwestern limb among the least decelerated ejecta suggesting a convergence date of $1681 \pm 19$. A remnant age of around 325 yr would imply a $\simeq 350$ km s$^{-1}$ transverse velocity for the central X-ray point source.

*Subject headings:* ISM: individual (Cassiopeia A) - supernova remnants ISM: kinematics and dynamics

## 1. INTRODUCTION

The relative roles of neutrino heating and bipolar MHD jets as the underlying mechanism behind core-collapse supernovae (SNe) are controversial (Janka et al. 2003; Wheeler 2003). However, despite current uncertainties about the specific engine that drives core-collapse explosions, a variety of observations and hydrodynamic modeling make a compelling case that high-mass SNe are intrinsically aspherical events.

Observations of extragalactic core-collapse SNe show increasing late-time linear polarization levels suggesting that the innermost layers driving the SN expansion are aspherical (Trammell et al. 1993; Wang et al. 1996, 2001; Leonard et al. 2000, 2001; Leonard & Filippenko 2001). In the case of SN 1987A, spectropolarimetric observations and the early detection of gamma-rays and hard X-rays indicating the transport of freshly synthesized $^{56}$Ni from the core to the H-rich envelope lead to a model of envelope asymmetries and ejecta fragmentation (Arnett et al. 1989; Chevalier & Soker 1989). Recent *Hubble Space Telescope* (*HST*) images of SN 1987A reveal an elongated, axially symmetric remnant (Wang et al. 2002).

State-of-the-art numerical simulations also show that spherically symmetric core-collapses do not yield successful explosions (Rampp & Janka 2000; Liebendörfer et al. 2001, 2005; Buras et al. 2003; Thompson et al. 2003). This has lead some modelers to investigate the effects of rapid rotation and magnetic fields leading to magnetorotational jet models (Symbalisty 1984; Khokhlov et al. 1999; Wheeler et al. 2000; Höflich et al. 1999, 2001; Akiyama et al. 2003). Others have investigated asymmetric neutrino-driven models in order to generate aspherical sometimes even jet-like SN explosions (Burrows et al. 1995; Shimizu et al. 2001; Kifonidis et al. 2003; Madokoro et al. 2004; Janka et al. 2005; Yamasaki & Yamada 2005; Wilson et al. 2005). Asymmetries in either the neutrino heating or MHD jets might also explain pulsar 'kick' velocities (Fryer 2004; Scheck et al. 2004; Kotake et al. 2005).

Observations of 'long-duration' gamma-ray bursts (GRBs) suggest highly aspherical core-collapse explosions. In the popular 'collapsar' GRB model, a high mass core-collapse SN creates a black hole generating bipolar relativistic jets (Woosley 1993;

[1] Based on observations with the NASA/ESA Hubble Space Telescope, obtained at the Space Telescope Science Institute, which is operated by the Association of Universities for Research in Astronomy, Inc. under NASA contract No. NAS5-26555.

[2] 6127 Wilder Lab, Department of Physics & Astronomy, Dartmouth College, Hanover, NH 03755
[3] Department of Physics and Astronomy, Arizona State University, Box 871504, Tempe, AZ 85287
[4] Department of Astronomy, University of Virginia, P.O. Box 3818, Charlottesville, VA 22903
[5] Department of Physics, North Carolina State University, Raleigh, NC 27695
[6] Research School of Astronomy and Astrophysics, The Australian National University, Cotter Road, Weston Creek, ACT 2611 Australia
[7] Astrophysics Group, Imperial College London, Blackett Laboratory, Prince Consort Road, London SW7 2BZ
[8] Department of Physics and Astronomy, Hofstra University, Hempstead, NY 11549
[9] Harvard-Smithsonian Center for Astrophysics, 60 Garden Street, Cambridge, MA 02138
[10] Dominion Astrophysical Observatory, Herzberg Institute of Astrophysics, NRC of Canada, 5071 West Saanich Road, Victoria, BC V9E 2E7, Canada

MacFadyen & Woosley 1999; MacFadyen et al. 2001). These jets excite an external shock from which energetic electrons, created through interaction with the ambient medium, radiate synchrotron emission giving rise to broadband afterglows. Direct connections between SNe and GRBs include the observational coincidences between GRBs and SN 1998bw and SN 2003dh, 'bumps' in some GRB afterglow light-curves consistent with underlying SN explosions (Galama et al. 1998; Hjorth et al. 2003; Stanek et al. 2003; Matheson et al. 2003; Kawabata et al. 2003; Malesani et al. 2004; Mazzali et al. 2005), and indications that GRBs are related to star forming regions (Paczynski 1998; Fruchter et al. 1999).

Compared to SN observations, evidence for aspherical SN explosions based on supernova remnant observations is much less clear. One of the most often cited asymmetrically expanding SNRs is that of Cassiopeia A (Cas A), currently the youngest known (∼300 yr) Galactic, core-collapse remnant. On even the earliest photographic plate images, a 'flare' or 'jet' of knots and filaments could be seen extending out along the northeast limb about $3.8'$ from the remnant center at a PA $\sim 70°$ (Minkowski 1968; van den Bergh & Dodd 1970). Whereas the main $\simeq 2'$ radius emission ring of ejecta expands at velocities $4000 - 6000$ km s$^{-1}$, debris in the NE jet have estimated velocities more than twice as large, up to 14000 km s$^{-1}$ (Fesen & Gunderson 1996; Fesen 2001). However, both the main shell's so-called 'Fast-Moving Knots' (FMKs) and NE jet ejecta knots have similar emission line spectra; namely, strong lines of [S II] $\lambda\lambda$6716,6731, suggesting similar chemical make-ups. A southwest 'counterjet' of high-velocity, [S II] emitting ejecta was recently discovered (Fesen 2001) and confirmed in X-rays and the infrared (Hwang et al. 2004; Krause et al. 2005).

While the presence of a jet and counterjet in this high-mass progenitor SNR might indicate an aspherical SN expansion, the nature of these jet features is controversial. Proposed explanations include uneven ejecta decelerations due to local ISM density variations and cavities (Minkowski 1968; Blondin et al. 1996, 2001), bipolar MHD jets (Khokhlov et al. 1999; Wheeler et al. 2002), or mildly asymmetrical neutrino-driven explosions (Janka et al. 2005; Burrows et al. 2005). Complicating matters, the NE and SW jets are not the only outlying ejecta around Cas A, with several dozen high-velocity, nitrogen-rich knots located in other regions of the remnant (Fesen, Becker, & Blair 1987; Fesen 2001).

In this paper, we report results from a deep *HST* imaging survey of the Cas A SNR. These images reveal a large population of high-velocity knots of ejecta with an asymmetric distribution. A complete catalog of outer ejecta knots will be presented in a separate paper (Hammell & Fesen 2006). Here we address the overall spatial distribution and expansion velocity of the remnant's outer ejecta and discuss limits on the dynamical age of the remnant. The observations and knot flux measurement procedures are described in §2 and §3, with the results presented and discussed in §4 and §5, respectively.

## 2. OBSERVATIONS

High resolution *HST* images of the Cas A remnant were obtained on 4–6 March 2004 and 4–5 December 2004 using the Wide Field Channel (WFC) of the Advanced Camera for Surveys (ACS; Ford et al. 1998; Pavlovsky et al. 2004). The ACS/WFC consists of two $2048 \times 4096$ CCDs with an average image pixel scale of $0\farcs05$ providing a $202'' \times 202''$ field of view. Four 2-point line dithered images were taken in each of the four ACS/WFC Sloan Digital Sky Survey (SDSS) filters, namely F450W, F625W, F775W, and F850LP (i.e., SDSS g,r,i, and z), at each target position to permit cosmic ray removal, coverage of the $2\farcs5$ interchip gap, and to minimize saturation effects of bright stars in the target fields.

Total integration times in the F450W, F625W, F775W, and F850LP filters were 2000 s, 2400 s, 2000 s, and 2000 s, respectively. Standard pipeline IRAF/STSDAS[11] data reduction was done including debiasing, flat-fielding, geometric distortion corrections, photometric calibrations, and cosmic ray and hot pixel removal. The STSDAS *drizzle* task was used to combine exposures in each filter. Due to significant reddening toward Cas A ($A_V = 4.5 - 8$ mag; Hurford & Fesen 1996; Reynoso & Goss 2002), [O III] $\lambda\lambda$4959,5007 line emission was too weak to be detected for most outlying knots and we have not included F450W images in our analysis.

We measured outer knot ACS/WFC fluxes from the three remaining SDSS filter image sets using the automated source extraction software package SExtractor (Bertin & Arnouts 1996). In cases where the SExtractor program failed to return a reasonable flux or failed to return a flux at all, the knot fluxes were calculated by hand. In all cases, the fluxes were calculated using 5 pixel apertures. Background estimates were performed by SExtractor using a 24 pixel rectangular annulus about the isophotal limits of the object. When fluxes were calculated manually, background estimation was performed by calculating the total 5 pixel aperture flux in at least five positions near the object (avoiding other sources) and then subtracting the mean computed "background" flux from the total object pixel sum. Most knots whose fluxes required manual computation were located near a bright background source or very close to another ejecta knot.

## 3. OUTER KNOT IDENTIFICATION AND FLUXES

High-velocity, outer ejecta knots were identified through proper motion measurements on the March and December 2004 ACS/WFC images (Hammell & Fesen 2006). Ejecta knots were defined as being high-velocity if their epoch 2004.3 radial distance exceeded $100''$ from the remnant's center of expansion ($V_{exp} \sim 5500$ km s$^{-1}$) and they showed a proper motion $\geq 0\farcs35$ yr$^{-1}$ (see Hammell & Fesen 2006).

Following Hammell & Fesen (2006) and Fesen et al. (2006), we used the filter fluxes to bin outlying ejecta knots into three emission classes; namely, strong [N II] $\lambda\lambda$6548,6583 emission knots, strong [O II] $\lambda\lambda$7319,7330 emission knots, and strong [S II] $\lambda\lambda$6716,6731 FMK-like knots. Flux ratio criteria between these three classes were chosen to segregate knots with similar ra-

[11] IRAF is distributed by the National Optical Astronomy Observatories, which is operated by the Association of Universities for Research in Astronomy, Inc. (AURA) under cooperative agreement with the National Science Foundation. The Space Telescope Science Data Analysis System (STSDAS) is distributed by the Space Telescope Science Institute.

tios seen for main shell or outer ejecta knots with existing spectroscopic data. For example, outlying ejecta knots whose 5000 − 7500 Å spectra show largely just [N II] λλ6548,6583 emission like those discussed by Fesen (2001) exhibit F625W/F775W and F625W/F850LP ratios more than an order of magnitude larger than [S II] bright knots. In similar fashion, the newly discovered outlying O-rich knots which show a 6000 - 7500 Å spectrum with strong [O I] and [O II] line emissions (Fesen et al. 2006), exhibit the O/S sensitive F775W/F850LP ratio several times greater than even strong [O II] λλ7319,7330 emission main shell knots.

Specifically, we chose a flux ratio for F775W/(F625W + F850LP) ≥ 1.0 to separate out the [O II] strong FMKs from the [S II] strong FMKs; that is, those knots with stronger [O II] λλ7319,7330 emission detected via the F775W filter than the combined strength of [N II], [S III] and [S II] emissions detected in the F625W and F850LP filters.

Similarly, knots with strong [N II] emissions were selected via F625W/(F775W + F850LP) ≥ 1.0, thereby selecting those knots where the combined flux of [O I] λλ6300,6364, [S II] λλ6716,6731, and [N II] λλ6548,6583 emissions was greater than the sum of F775W flux, due mostly to [O II], and F850LP flux sensitive to the near-infrared [S III] and [S II] emissions. Since [O I] λλ6300,6364 flux rarely, if ever, exceeds the [O II] λλ7319,7330 flux, and the observed [S II] λλ6716,6731 emission is unlikely to ever exceed the combined flux of [S III] λλ9069,9531 plus [S II] λλ10287–10370 line emissions (Hurford & Fesen 1996; Winkler et al. 1991), then any knot for which the F625W/(F775W + F850LP) ≥ 1.0 requires the presence of significant [N II] λλ6548,6583 emission.

## 4. RESULTS

Examination of March and December 2004 ACS/WFC images revealed a total of 1825 high proper motion ($\mu \geq 0\farcs35 - 0\farcs90$ yr$^{-1}$) ejecta knots around the Cas A remnant (Hammell & Fesen 2006). This is a much larger population of high-velocity ejecta knots than previously identified or suspected from ground-based images (Kamper & van den Bergh 1976; Fesen & Gunderson 1996; Fesen 2001). A total of 444 strong [N II] emission, 192 strong [O II] emission, and 1189 FMK-like knots were identified. Although nearly half of the 1825 cataloged outer knots were found in the NE jet, high-velocity outlying ejecta were identified in many other regions around the remnant.

Outlying optical ejecta knots range from 105″ to 300″ in radial distance from the center of expansion, placing them in projection close to or outside the remnant's ≃ 6000 km s$^{-1}$ forward shock front as determined by the remnant's outermost X-ray emission (Gotthelf et al. 2001; DeLaney & Rudnick 2003). The location and distribution of these knots with respect to the remnant's outer X-ray emission filaments associated with the forward shock front can be seen in Figure 1. Here we show the locations of all 1825 cataloged outer knots projected onto the 1 Msec *Chandra* ACIS image (epoch 2004.3; Hwang et al. 2004). Knot positions are marked with open circles color coded either red, green, or blue to indicate those knots with spectra dominated by strong [N II] λλ6548,6583, [O II] λλ7319,7330, or [S II] λλ6716,6731 line emissions, respectively.

The transverse expansion velocities of Cas A's outermost ejecta (Fig. 1) show a strongly aspherical structure due principally to the NE and SW jets which appear as distinct and roughly opposing features; NE jet: P.A. = 45° − 70°, SW jet: P.A. = 230° − 270°. The jets have similar maximum radial distances and proper motion derived expansion velocities; namely $r = 290'' - 300''$ and $v$ = 14000 km s$^{-1}$. They also contain the remnant's highest velocity [S II] emitting ejecta (the blue open circles in Fig. 1). This is in contrast to other regions where the nitrogen-rich ejecta (open red circles) represent the remnant's highest velocity debris (10000 − 11000 km s$^{-1}$) followed by the O-rich ejecta, and then the S-rich knots (Fesen et al. 2006).

Examination of the *HST* images also revealed a lack of outlying ejecta knots along the remnant's northern and southern regions. Not a single ejecta knot could be found along a 55° wide region in position angle along the remnant's southern limb (i.e., PA = 145° − 200°) and in a narrower 15° position angle zone along the north (PA = 335° − 350°). The northern gap would actually be larger if one only considered knots with radial distances greater than 180″ in which case the northern gap size grows to ∼ 35° in position angle (PA = 327° − 3°). We note that, unlike for the northern limb region, ACS images did not completely cover the whole southern limb region imaging only out to a distance of 180″ due south of the center of expansion. However, inspection of ground-based images covering regions farther to the south (∼ 200″) revealed no bright farther outlying knots. Thus, despite missing ACS/WFC coverage along the south, the lack of any knots at smaller distances like those seen along the east and west edges of the southern gap (r = 150″ − 185″) indicate a strong likelihood that there are simply no bright, high-velocity ejecta knots in either of the NNW and SSE directions.

This NE–SW jet/counterjet and NNW–SSE gap asymmetry in the distribution of the remnant's outer optical ejecta knots can be clearly seen in the proper motion plots of Figure 2. In the top panel, we plot the extrapolated 320 yr proper motion paths for the 1825 identified outer knots based on measured March to December 2004 positions. The central white circle has a radius of 5″ centered on the remnant's estimated center of expansion (COE; $\alpha$(J2000) = $23^{\rm h}23^{\rm m}27\fs77 \pm 0\fs05$, $\delta$(J2000) = $58°48'49\farcs4 \pm 0\farcs4$; Thorstensen et al. 2001). Although errors in derived knot proper motions lead to some knot trajectories missing the expansion center by substantial distances filling in somewhat the northern and southern gaps, a strongly aspherical distribution of ejecta jets and gaps is readily apparent.

When the proper motion extrapolations are replaced with predicted knot proper motions based solely on March 2004 knot positions and the COE, a structure of opposing jet features and north and south gaps appears even more striking (Fig. 2, bottom panel). The circle in the figure marks a radial distance of 200″ from the COE corresponding to a proper motion of $0\farcs625$ yr$^{-1}$ for an age of 320 years and an implied ≃10,000 km s$^{-1}$ transverse velocity assuming a remnant distance of 3.4 kpc. As can be seen from the figure, this circle encompasses nearly all the remnant's N-rich outer ejecta away from the jet regions.

Peak NE and SW jet optical knot transverse velocities lie at PA = 60° − 61° and at PA = 238° − 243°, respectively, i.e., ≃180° apart. These position angles are close to those seen also in the X-rays and infrared for the NE and SW jets. That is, from the 1 Ms *Chandra* (Hwang et al. 2004) and 24 micron *Spitzer* images (Krause et al. 2005), we find PA = 63°–65° for the center of the NE jet and PA = 246°–248° for the center of the SW jet, some 183° apart. While the significance of the northern and southern gaps in the distribution of the outer knots is uncertain (see below), they are situated roughly orthogonal to this NE–SW jet alignment line. The middles of the southern and northern outer knot gaps lie at PA = 170° and 342° respectively, some 107° and 99° off from a 63°–243° alignment line.

Lastly, extrapolated late 17th century knot positions relative to the remnant's estimated COE indicates some evidence for non-uniform deceleration around the remnant. Figure 3 (left panel) shows the estimated positions for all 1825 outer knots for the Thorstensen et al. (2001) estimated convergent year 1671. The estimated COE is marked by the circle (radius = 5″). Here, one sees that the scatter of points for the outer knots is significantly away from the Thorstensen et al. (2001) center, centered instead 3.″4 to the east. (Note: A check using the same 17 outer knots employed by Thorstensen et al. (2001) using the new ACS images together with archival images agree with their derived COE.) One possible cause for this shift eastward is a greater deceleration of knots along different regions around the remnant, particularly along the eastern limb, giving rise to broader and slower average expansion velocities for a given radial distance and look-back time. A different shift off from the COE is seen when plotting just northern and southern knots (Fig. 3; right panel). For 416 north and south knots, the shift from the COE shows an even greater displacement, namely 5.″2 to the southeast.

## 5. DISCUSSION

Although optical debris may constitute only a small fraction of the total ejected mass, Cas A's fastest moving material is perhaps best studied optically. For example, optical emission from the NE and SW jets can be traced about 80″ farther out than in X-rays or infrared (Hwang et al. 2004; Krause et al. 2005) and only a handful of outer optical ejecta knots around the rest of the remnant are detected in even the deepest radio or X-ray images.

Fragmentation of SN ejecta into dense clumps may come about by Rayleigh-Taylor instabilities brought on by the deceleration of the ejecta by the ambient medium (Gull 1975; Jones et al. 1994; Jun et al. 1996), passage of the reverse shock (Herant & Woosley 1994), or inside the progenitor during the SN explosion (Chevalier 1975; Chevalier & Klein 1978). Optical emission will arise when ∼100 km s$^{-1}$ internal shocks are formed in the clumps driven by the high stagnation pressure behind the clump's bow shock.

Hamilton (1985) studied similarity solutions for SN blast waves driven by clumpy ejecta and found that such clumps will eventually move ahead of a remnant's forward shock front. He concluded that this process may be a generic feature of SNRs with clumped ejecta. The presence of numerous dense and relatively cool optically emitting, high-velocity ejecta knots out ahead of Cas A's forward shock front supports Hamilton's basic results. Namely, we find a significant number of optical outer ejecta knots lying (in projection) outside the faint X-ray emitting filaments marking the current location of the remnant's forward blast wave (Gotthelf et al. 2001; DeLaney & Rudnick 2003).

### 5.1. *Asymmetrical Expansion*

Asymmetries in Cas A's outermost debris may offer clues as to the nature of the SN explosion engine. What one observes at a particular epoch, however, may not necessarily reflect the SN's true explosion dynamics. Ejecta velocities will be modified (to varying degrees) by passage through the ambient medium as ejecta knots are only made optically visible due to this interaction, and more knots will be visible in regions where there is more circumstellar material.

The detected distribution can also change with time since some 10–20% of outer optical knots vary significantly in brightness over just a few years due presumably to variable interaction with a clumpy CSM (Hammell & Fesen 2006). In addition, for a knot to be visible it must be sufficiently large and dense to generate detectable forbidden line emission. It must also survive disruption via mass ablation from Kelvin-Helmhotz instabilities during passage through the reverse shock, forward shock, and the surrounding ambient medium. Consequently, what one sees can be a distorted and biased view of the true distribution of a remnant's outer debris.

Nonetheless, even with all these caveats, the asymmetry and non-uniformity of the remnant's outermost optical ejecta as seen in the plots of Figure 2 is striking. The NE and SW jets extend out to nearly 300″, more than twice the radius of the remnant's main emission shell, and lie on virtually opposite sides of the remnant's center of expansion. The jets also appear to lie roughly in the plane of the sky to within ∼ 30° (Minkowski 1968; Fesen & Gunderson 1996; Fesen 2001). This combination of an opposing, sulfur-rich jet/counterjet structure with similar maximum expansion velocities plus gaps of high-velocity ejecta aligned roughly perpendicular is suggestive of an aspherical, bipolar expansion.

From 2-D models, Blondin et al. (1996) calculated that a progenitor's axisymmetric wind structure, where the highest density lay in the equatorial plane, could generate bipolar protrusions of SN ejecta extending $2-4$ times the radius of the main shell. The relative scale of such expansion asymmetry is not unlike that seen in the Cas A jets and only a mild asymmetry ($\rho_e/\rho_p \sim 2$) is needed to form obvious protrusions. While significant heavy element material can end up at much larger radial distances than elsewhere, the original progenitor chemical layering should largely persist within the protrusion. That is, the highest velocity material should mainly exhibit the chemical abundances of the progenitor's outermost layers, namely N, He, and O. However, just the opposite is observed. The farther out one goes in either of Cas A's jets, the weaker oxygen emission lines become relative to those of sulfur (van den Bergh 1971; Fesen & Gunderson 1996; Fesen 2001).

The fact that one sees largely undecelerated ejecta throughout the remnant with $v \propto r$ (see Fesen et al. 2006) indicates that the observed compositional struc-

ture is set early in the explosion. In addition, outside of the jet regions, the S-rich material has a much more limited velocity range. All this suggests that the S-rich NE jet, rather than reflecting some sort of turbulent mixing region or a rapid expansion into surrounding ISM/CSM due to a lower surrounding density, more likely represents a true stream of high-speed ejecta formed when underlying material was ejected up through the star's outer layers.

Other observational evidence in favor of an ejection of underlying material comes from the location of the so-called 'mixed ejecta knots' and from energy estimates in the jet region. Mixed ejecta knots show both nitrogen and sulfur overabundances, which could have resulted from turbulent mixing of H and N-rich layers with underlying S and O-rich layers, are only seen in the jet regions (Fesen & Becker 1991; Fesen 2001). The ACS/WFC images show that many of the mixed knots are not the result of line-of-sight superposition of knots with different chemical make-up but appear to be ejecta with mixed chemical properties (Hammell & Fesen 2006). In addition, from an analysis of *Chandra* X-ray data, Laming & Hwang (2003) found a shallower outer envelope near the base of the NE jet which they interpreted as indicating more of the initial explosion's energy being directed in this polar direction as opposed to equatorial. On the other hand, however, while the prominent shell rupture near the base of the NE jet seen in X-rays and radio images might be seen as supporting evidence for this picture (Fesen & Gunderson 1996), there is no obvious main shell rupture near the SW counterjet.

### 5.2. *Jet/Counterjet: MHD or Neutrino Driven?*

Although our *HST* survey of the highest-velocity ejecta in Cas A makes a compelling case for a high-velocity bipolar expansion, what the jets and gaps are telling us about the underlying core-collapse mechanism is unclear.

Currently, there is no consensus as to the details of the explosion process for core-collapse SNe except that models with completely spherical neutrino heating mechanisms fail to yield successful explosions (Rampp & Janka 2000; Liebendörfer et al. 2001, 2005; Thompson et al. 2003). This has led to considerable effort to understanding the effects of rotation on neutrino heating and the importance of magnetic fields in the proto-neutron star.

Around the rotation axis of a collapsing star, accretion flow will be non-spherical and accelerated thereby lowering the needed critical neutrino luminosity (Yamasaki & Yamada 2005). The degree of neutrino re-vitalization of the shock front created by the core-bounce may also be affected by convection in the proto-neutron star through the mechanical outward transfer of neutrinos. Investigations into the effects of rotation on the anisotropic neutrino emission from the proto-neutron star indicate a weakening of the core bounce that seeds the neutrino-drive convection, with angular momentum tending to stabilize the core, constraining convection to the polar regions (Fryer & Heger 2000; Burrows et al. 2004). Models of anisotropic neutrino radiation indicate more powerful explosions are generated, which then lead to a prolate expansion geometry (Shimizu et al. 2001; Madokoro et al. 2003, 2004; Wilson et al. 2005). Walder et al. (2005) found the bipolar expansion was not strongly collimated ($\sim 30^\circ - 60^\circ$) unless the rotation rate was large.

For Cas A, Burrows et al. (2004, 2005) favored a rotation enhanced, neutrino-driven model in which the X-ray observed Fe-rich SE and NW regions, and not the NE and SW jet/counterjet, mark the progenitor's rotation axis. Instead of driving the explosion, the NE–SW jets would have formed following the neutrino-driven main explosion via an under-energetic jet-like ejection created by an MHD jet or proto-neutron star wind (possibly associated with accretion by the NS; Janka et al. 2005) emerging into an already expanding debris field. But this model requires a nearly 90° post-explosion precession of the NS's rotation axis from NW–SE to NE–SW (Burrows et al. 2004, 2005), the cause of which is left unexplained.

On the other hand, models of magnetorotationally induced jets capable of generating SN explosions have also been invoked to explain the Cas A jets (Khokhlov et al. 1999; Wheeler et al. 2000, 2002; Akiyama et al. 2003; Takiwaki et al. 2004). In this view, rotation leads to magnetic field amplification thereby generating non-relativistic axial jets of MHD energy $\sim 10^{51-52}$ erg which then initiate a bipolar supernova explosion. This is somewhat analogous to the narrow relativistic jets proposed in the collapsar model as the central engine for GRBs. Kifonidis et al. (2003) questioned the accuracy of anisotropic jet explosion simulations and Janka et al. (2005) argue that if the Cas A jets were driven by outflowing core material they should be Fe-rich instead of the S and Si rich material observed.

If Cas A's NE and SW jets were driven by Ni-rich material, the energy deposited by radioactive $^{56}$Ni decay might have created hot, low density Ni-rich bubbles. This could make Fe-rich material in the jets today too cool for detection in X-rays while also being too diffuse and low density to detect as optically bright knots. Furthermore, while both the NE and SW jets can be traced farthest out in the optical, optical studies have never detected appreciable Fe-rich material anywhere in Cas A. Optical Fe line emissions are weak and hard to detect in even the brightest main shell knots and there is no optical Fe-rich material seen corresponding to the Fe-rich SE and N regions observed in the X-rays (Winkler et al. 1991; Reed et al. 1995; Hurford & Fesen 1996).

Morphologically, both MHD jet and neutrino-driven expansion models produce aspherical 'jets' with axial expansion ratios around 2 like those seen for Cas A (Khokhlov et al. 1999; Kotake et al. 2005). Although much of the NE jet's central and farthest extending line of optical filaments lie virtually in the plane of the sky (Minkowski 1968; Fesen & Gunderson 1996), knots lying at a projected radial distance of 150–170 arcsec out from the COE show radial velocities from $-3000$ to $+5000$ km s$^{-1}$, indicating an expansion cone about 25° wide (Fesen & Gunderson 1996). This means that the NE jet is more like a fan of several streams of ejecta knots (rather than a single narrow jet), about as deep as it appears wide, i.e., about $\sim 25^\circ - 35^\circ$. This is consistent with their appearance on X-ray and infrared images which show both jets as two or three ejecta streams rather than one single narrowly focused line of emission. For example, there are three main optical lines of knots in the NE jet which correlate with X-ray and IR emission fingers. Although the SW jet is optically much less well-defined, the locations of the outermost [S II] emitting ejecta cor-

relate reasonably well with the X-ray and IR emission 'fingers'.

Beside the jets, a possible additional clue as to the nature of the central core-collapse SN engine may be the absence of high-speed ejecta along the north and south limbs. Not all proposed core-collapse models show a pronounced decrease in outermost expansion velocity suggested by the nearly opposing ejecta gaps revealed in the *HST* data (Fig. 2). However, similar gaps in the distribution of slower moving ejecta are not found in the remnant's main emission ring of reverse shocked debris based on radio, X-ray, and optical maps. While the remnant's forward shock shows no decrease in these directions as one might expect if the expansion velocity was significantly lower in these northern and southern gap regions (Gotthelf et al. 2001), a gap in the forward shock front would be rapidly filled by the blast wave advancing in from the sides. Thus, while the north and south ejecta gaps are interesting especially given their positions relative to the jets, their meaning is presently unclear. Nevertheless, if these gaps are truly found to be areas devoid of high-speed ejecta seen elsewhere around the remnant and orthogonal to the NE/SW jets they may provide some insight for testing core-collapse models.

### 5.3. *Motion of Central X-ray Point Source*

First-light images of Cas A taken by the *Chandra* X-ray Observatory revealed a central X-ray point source (XPS) in the remnant (Tananbaum 1999). Although its nature is uncertain, this object is likely to be a neutron star but not a pulsar due to a lack of radio pulsations, no detected X-ray or radio plerion, and an X-ray spectrum too steep for an ordinary pulsar (Pavlov et al. 2000). It has been suggested that it may be a younger and less luminous example of a subclass of neutron stars known as anomalous X-ray pulsars (AXPs) and soft gamma-ray repeaters (SGRs) (Chakrabarty et al. 2001; Mereghetti, Tiengo, & Israel 2002; Pavlov et al. 2002; Rothschild & Lingenfelter 2003; Pavlov et al. 2004; Fesen, Pavlov, & Sanwal 2006). X-ray emission bursts from AXPs and SGRs together with their spin-down rates have been explained by a magnetar model in which a neutron star has a much higher surface magnetic field of $10^{14} - 10^{15}$ G than ordinary pulsars (Duncan & Thompson 1992; Thompson & Duncan 1996). Except for a lack of pulsations, the general properties of the Cas A XPS and other X-ray emitting but radio quiet compact central objects in fairly young SNRs are not all that dissimilar from AXPs and SGRs (Pavlov et al. 2002; Fesen, Pavlov, & Sanwal 2006).

Core-collapse asymmetries in the SN explosion might help explain the inferred high space velocities (200 – 500 km s$^{-1}$ or more) for neutron stars and radio pulsars (Lyne & Lorimer 1994; Cordes & Chernoff 1998; Brisken et al. 2003). Although 3D core-collapse models suggest neutrino asymmetries as well as disruption of binaries by symmetric explosions may be insufficient to generate the wide range of observed 'kick' pulsar velocities (Cordes & Chernoff 1998; Fryer 2004), MHD driven explosions creating unbalanced jets just might (Khokhlov et al. 1999).

However, the motion of the remnant's XPS is far from being in alignment with Cas A's NE–SW jets. Using the initial *Chandra* derived position along with subsequent positional measurements using archival *ROSAT* and *Einstein* image data (Aschenbach 1999; Pavlov & Zavlin 1999), Thorstensen et al. (2001) estimated a 6.″6 displacement of the XPS from their derived center of expansion. Assuming a common origin for the XPS and the expanding ejecta, they estimated a transverse velocity of ≈330 km s$^{-1}$ for a distance of 3.4 kpc. Adopting an updated position of the XPS (2004 epoch; Fesen, Pavlov, & Sanwal 2006), the displacement of the XPS from the Thorstensen et al. (2001) remnant expansion center is 7.″0±0.″8 with an implied motion in a southeasterly direction (position angle = 169° ± 8.4°; see Fig. 4, left panel). Assuming a current remnant age ≃ 325 yr (see discussion in §5.4), we find a slightly higher transverse velocity of around 350 km s$^{-1}$ for a distance of 3.4 kpc.

The apparent southernly direction of motion for the XPS is roughly orthogonal to the jet-counterjet alignment line, making an asymmetric jet-induced 'kick' explanation problematic. Interestingly however, the projected motion of the XPS is toward the middle of the broad southern gap in the distribution of the outer ejecta knots (Fig. 4; right panel). If the distribution of the optically emitting outer ejecta knots is giving us a true picture of the asymmetry in the Cas A supernova expansion, then the neutron star's preference to move in a direction lacking in high velocity material may indicate a natal kick aligned with the progenitor's slowest velocity expansion, possibly the progenitor's equatorial region.

Duncan & Thompson (1992) and Arras & Lai (1999) have proposed that magnetars could receive natal kicks in part due to their intense magnetic fields which could lead to anisotropic neutrino emissions. However, unlike the case seen here for Cas A, these kicks would be in the direction of the rotation axis – which the NE–SW jets would seem to mark. While some misalignments between the progenitor's spin axis and a neutron star's velocity vector have been reported (Hughes & Bailes 1999), including the high velocity pulsar B1508+55 ($V_{trans}$ ≃ 1100 km s$^{-1}$; Chatterjee et al. 2005), there is not strong observational evidence for general misalignments (Deshpande et al. 1999). Moreover, although some binary disruption type models have been proposed to explain natal kicks perpendicular to the spin axis (e.g., Wex et al. 2000; Colpi & Wasserman 2002), no clear picture has emerged on how such a misalignment would be produced or even whether such models apply to the case of Cas A.

### 5.4. *Dynamical Age Estimates for Cas A*

Although only nine months separated the two sets of ACS/WFC images, the large number of outer knots identified (1825) permitted us to estimate the dynamical age of the Cas A SNR. Assuming the COE derived by Thorstensen et al. (2001) and no knot deceleration since the time of the explosion, we show in Figure 5 (left panel) the estimated arrival date of the 1825 cataloged outlying ejecta knots to within the minimum least squared distance to the COE plotted versus cataloged knot identification number (Hammell & Fesen 2006). In this figure, symbol size is inversely proportional to estimated proper motion uncertainty. Knot catalog IDs are in order of increasing position angle with the NE jet knots (ID numbers ∼ 100 – 950) making up a substantial fraction

(∼45%) of the 1825 cataloged knots.

The dispersion in estimated knot convergent dates is not uniform as a function of position angle. For example, for the middle section of the NE jet where many of the fastest ejecta are found (i.e., Knot IDs 350 − 550), a decrease in the range of estimated knot arrival dates can be seen in Figure 5 (left panel). This decrease reflects more accurate proper motion values due mainly to the larger radial distances for jet knots from the COE and consequently larger proper motion values leading to smaller percentage measurement errors.

#### 5.4.1. *Age Estimates Assuming No Knot Deceleration*

The average arrival date for the 1825 outer knots with undecelerated extrapolated arrival dates between 1580 and 1750 is 1662±27 yr. This is consistent with that estimated by Thorstensen et al. (2001) who found an undecelerated convergent date of 1671.3±0.9 based on a sample of 17 especially long-lasting knots for which archival imaging data were available covering a time span of up to 50 years. Because the catalog of 1825 outer knots covered a wide range of sizes and brightnesses leading to a range of proper motion measurement errors, we examined a much smaller, hand-selected sample of 72 knots which are: i) relatively bright, and ii) compact in size or unresolved in the ACS/WFC images. This sample included the 17 outer knots used by Thorstensen et al. (2001) for their estimated convergent date. The results for this smaller sample, shown in Figure 5 (right panel), indicate a convergent date 1671.8 ± 17.9, in excellent agreement with the Thorstensen et al. 1671 date, shown here as a vertical dashed line.

#### 5.4.2. *Knot Deceleration*

While ejecta knots must undergo shock heating and hence some deceleration in order to be optically visible, the least decelerated ones offer stronger upper limits to the remnant's age. As seen in Figure 5, the region near the top of the left-hand plot, i.e., knot IDs from 1690 − 1815 corresponding to position angles 275° − 315° respectively, show displacements toward a convergent date later than 1671, namely 1680.5 ± 18.7. These 126 knots are located along the remnant's northwest limb and can be seen in the bottom panel of Figure 2 as cluster of NW knots.

If we knew the degree of deceleration these northwestern limb knots might have experienced over the ∼300 yr age of the remnant, it would give us a better estimate of the remnant's age and therefore the actual Cas A SN explosion date. For example, if knot decelerations were significant then one might be able to rule out on dynamical grounds a proposed but controversial sighting of the Cas A SN by Rev. John Flamsteed in August 1680 (Ashworth 1980; Stephenson & Green 2002).

A knot will undergo deceleration both from the direct interaction with local gas as well as from the internal shock driven into the knot that gives rise to the optical emission observed (Jones et al. 1994). If treated as a dense undistorted clump, a knot's deceleration due to drag from its interaction with the ambient medium depends on knot velocity and mass, the density of the local medium, and the cross-sectional area of the knot's bow shock which for hypersonic conditions is approximately equal to the knot itself (Chevalier 1975; Hamilton 1985; Jones et al. 1994).

The timescale for knot deceleration (drag) is given by $\tau_{drag} \sim \chi R_k/v_k$ where $\chi$ is the density contrast between the knot and the ambient medium (i.e., $\rho_k/\rho_a$), $R_k$ is the knot's radius, and $v_k$ is the knot's velocity (Jones et al. 1994). Based on our ACS imaging data, typical outer knots have velocities of 10,000 km s$^{-1}$ and sizes R $\simeq 0\farcs1$ corresponding to 0.002 pc at 3.4 kpc. High-velocity outlying [S II] emitting knot electron densities lie between 2000 – 16,000 cm$^{-3}$ with typical values between 4000 – 10,000 cm$^{-3}$ (Fesen & Gunderson 1996; Fesen 2001). The ambient density around Cas A is not well determined but is estimated to range between 0.4 – 3.7 cm$^{-3}$ (Braun 1987).

Choosing a $\chi = 10^4$ and an outer ejecta knot velocity of 10,000 km s$^{-1}$ leads to $\tau_{drag} \sim 2000$ yr, suggesting that outer knot deceleration due to drag may be fairly small at present. This conclusion is consistent with a lack of detectable knot deceleration over the last 50 yr and a velocity change of $< 5\%$ over 300 yr (Thorstensen et al. 2001). While model simulations suggest that shocked clumps become flattened (i.e., laterally spread) which would increase their cross section and hence enhance the deceleration, radiative cooling might partially counteract this effect leading to clump breakup into a cluster of smaller, denser knots.

Cloud-ISM interaction models suggest knot disruption might also occur due to Rayleigh-Taylor and Kelvin-Helmholtz instabilities, again resulting in the generation of smaller, dense knot fragments (Klein et al. 1994; Jones et al. 1994; Cid-Fernandes et al. 1996). The timescale for initial knot breakup under these conditions, $\tau_b$, is uncertain but is likely to be a few 'cloud crushing times' (Klein et al. 1990; Jones et al. 1994) or $\tau_b \sim 4\ \chi^{1/2} R_k/v_k$. For the knot numbers assumed above, the disruption timescale is ∼ 50 yr, meaning the remnant's highest-velocity ejecta clumps might well have already undergone breakup into denser knots. Thus, both radiative cooling effects and dynamical instabilities might help explain the observed small-scale clustering of some of the remnant's outer ejecta knots (see Hammell & Fesen 2006).

Knot deceleration from internal shock passage will cause the largest error in convergent date if it has occurred recently, and given the $\sim 20 - 30$ year lifetimes of most optical knots in Cas A (Kamper & van den Bergh 1976), this is probably the case. The effective shock deceleration is equal to the internal knot shock velocity for post-shock emission (Dopita & Sutherland 1995). The shock speed must be at least 30 km s$^{-1}$ to produce significant [N II], [S II] and [O II] emissions (e.g.. Hartigan et al. 1994; Blair et al. 2000). Based on the Blair et al. (2000) shock models, shock speeds above about 500 km s$^{-1}$ will ionize the oxygen to the helium-like ionization state and higher, reducing the cooling rate by an order of magnitude. If the outer portions of the SNR are roughly in pressure equilibrium, the density is proportional to v$^{-2}$, further reducing the cooling rate behind fast shocks. Consequently, shocks above about 500 km s$^{-1}$ will have cooling times longer than the age of Cas A, and will appear as X-ray rather than optical emission features. Thus the observed knots have been

decelerated by 30 to 500 km $s^{-1}$, or 0.3 to 5% of their $\sim$10,000 km $s^{-1}$ apparent speeds. This corresponds to an error in convergence time of 0.003 to 0.05 times 320 yr, or 1 to 15 yr, well within the 19 yr uncertainty in the convergence time of the least decelerated northern limb knots.

We conclude that our convergence times estimates are not likely to be significantly affected by knot deceleration. Therefore, while the seemingly less decelerated knots located along the remnant's northern limb suggest an explosion date somewhat later than 1670, overall the measurements are still consistent with a possible sighting of the Cas A SN in 1680. Follow-up ACS imaging obtain in a few years may be able to settle this issue more definitely through a firmer estimate of the date for the Cas A supernova outburst.

This work was supported by NASA through grants GO-8281, GO-9238, GO-9890, and GO-10286 to RAF and JM from the Space Telescope Science Institute, which is operated by the Association of Universities for Research in Astronomy. RAC is supported by NSF grant AST-0307366 and CLG is supported through UK PPARC grant PPA/G/S/2003/00040.

REFERENCES


Akiyama, S., Wheeler, J. C., Meier, D. L., & Lichtenstadt, I. 2003, ApJ, 584, 954
Arnett, W. D., Fryxell, B. A., & Muller, E. 1989, ApJ, 341, L63
Arras, P., & Lai, D. 1999, ApJ, 519, 745
Aschenbach, B. 1999, IAU Circ. 7249
Ashworth, W. B. 1980, J. Hist. Astron., 11, 1
Bertin, E., & Arnouts, S. 1996, A&AS, 117, 393
Blair, W. P., et al. 2000, ApJ, 538, L61
Blondin, J. M., Lundqvist, P., & Chevalier, R. A. 1996, ApJ, 472, 257
Blondin, M. J., Featherstone, N., Borkowski, J. K., & Reynolds, P. S. 2001, Two Years of Science with Chandra Symposium, Washington, DC, September 2001, p166
Braun, R. 1987, A&A, 171, 233
Brisken, W. F., Fruchter, A. S., Goss, W. M., Herrnstein, R. M., & Thorsett, S. E. 2003, AJ, 126, 3090
Buras, R., Rampp, M., Janka, H.-T., & Kifonidis, K. 2003, Physical Review Letters, 90, 241101
Burrows, A., Hayes, J., & Fryxell, B. A. 1995, ApJ, 450, 830
Burrows, A., Ott, C. D., & Meakin, C. 2004, 'Cosmic Explosions in Three Dimensions, 209
Burrows, A., Walder, R., Ott, C. D., & Livne, E. 2005, ASP Conf. Ser. 332: The Fate of the Most Massive Stars, 332, 358
Bykov, A. M. 2003, A&A, 410, L5
Chakrabarty, D., Pivovaroff, M. J., Hernquist, L. E., Heyl, J. S., & Narayan, R. 2001 ApJ, 548, 800
Chatterjee, S., et al. 2005, ApJ, 630, L61
Chevalier, R. A. 1975, ApJ, 200, 698
Chevalier, R. A., & Klein, R. I. 1978, ApJ, 219, 994
Chevalier, R. A., & Soker, N. 1989, ApJ, 341, 867
Cid-Fernandes, R., Plewa, T., Rozyczka, M., Franco, J., Terlevich, R., Tenorio-Tagle, G., & Miller, W. 1996, MNRAS, 283, 419
Colpi, M., & Wasserman, I. 2002, ApJ, 581, 1271
Cordes, J. M., & Chernoff, D. F. 1998, ApJ, 505, 315
DeLaney, T., & Rudnick, L. 2003, ApJ, 589, 818
Deshpande, A. A., Ramachandran, R., & Radhakrishnan, V. 1999, A&A, 351, 195
Dopita, M. A., & Sutherland, R. S. 1995, ApJ, 455, 468
Duncan, R. C., & Thompson, C. 1992, ApJ, 392, L9
Fesen, R. A. 2001, ApJS, 133, 161
Fesen, R. A., & Becker, R. H. 1991, ApJ, 371, 621
Fesen, R. A., Becker, R. H., & Blair, W. P. 1987, ApJ, 313, 378
Fesen, R. A., & Gunderson, K. S. 1996, ApJ, 470, 967
Fesen, R. A., Hammell, M. C., Morse, J., Chevalier, R. A., Borkowski, K. J., Dopita, M. A., Gerardy, C. L., Lawrence, S. S., Raymond, J. C., & van den Bergh, S. 2006, ApJ, 636, 859
Fesen, R. A., Pavlov, G. G., & Sanwal, D. 2006, ApJ, 636, 848
Ford, H. C., et al. 1998, Proc. SPIE, 3356, 234
Fruchter, A. S., et al. 1999, ApJ, 519, L13
Fryer, C. L., & Heger, A. 2000, ApJ, 541, 1033
Fryer, C. L. 2004, ApJ, 601, L175
Galama, T. J., et al. 1998, Nature, 395, 670
Gotthelf, E. V., Koralesky, B., Rudnick, L., Jones, T. W., Hwang, U., & Petre, R. 2001, ApJ, 552, L39
Gull, S. F. 1975, MNRAS, 171, 263
Hamilton, A. J. S. 1985, ApJ, 291, 523
Hammell, M. C., & Fesen, R. A. 2006, in preparation
Hartigan, P., Morse, J. A., & Raymond, J. 1994, ApJ, 436, 125
Herant, M., & Woosley, S. E. 1994, ApJ, 425, 814
Hjorth, J., et al. 2003, Nature, 423, 847
Höflich, P., Wheeler, J. C., & Wang, L. 1999, ApJ, 521, 179
Höflich, P., Khokhlov, A., & Wang, L. 2001, AIP Conf. Proc. 586: 20th Texas Symposium on Relativistic Astrophysics, 586, 459
Hughes, A., & Bailes, M. 1999, ApJ, 522, 504
Hurford, A. P., & Fesen, R. A. 1996, ApJ, 469, 246
Hwang, U., et al. 2004, ApJ, 615, L117
Janka, H.-T., Buras, R., Kifonidis, K., Plewa, T., & Rampp, M. 2003, From Twilight to Highlight: The Physics of Supernovae, 39
Janka, H. -., Scheck, L., Kifonidis, K., Mueller, E., & Plewa, T. 2005, ASP Conf. Ser. 332: The Fate of the Most Massive Stars, 332, 372
Jones, T. W., Kang, H., & Tregillis, I. L. 1994, ApJ, 432, 194
Jun, B.-I., Jones, T. W., & Norman, M. L. 1996, ApJ, 468, L59
Kamper, K. & van den Bergh, S. 1976, ApJS, 32, 351
Kawabata, K. S., et al. 2003, ApJ, 593, L19
Khokhlov, A. M., Höflich, P. A., Oran, E. S., Wheeler, J. C., Wang, L., & Chtchelkanova, A. Y. 1999, ApJ, 524, L107
Kifonidis, K., Plewa, T., Janka, H.-T., & Müller, E. 2003, A&A, 408, 621
Klein, R. I., McKee, C. F., & Colella, P. 1994, in Evolution of the Interstellar Medium, ed. L. Blitz (Berkeley: ASP), 117
Klein, R. I., McKee, C. F., & Colella, P. 1994, ApJ, 420, 213
Kotake, K., Yamada, S., & Sato, K. 2005, ApJ, 618, 474
Krause, O. et al. 2005, Science, 308, 1604
Laming, J. M., & Hwang, U. 2003, ApJ, 597, 347
Leonard, D. C., Filippenko, A. V., Barth, A. J., & Matheson, T. 2000, ApJ, 536, 239
Leonard, D. C., Filippenko, A. V., Ardila, D. R., & Brotherton, M. S. 2001, ApJ, 553, 861
Leonard, D. C., & Filippenko, A. V. 2001, PASP, 113, 920
Liebendörfer, M., Mezzacappa, A., Thielemann, F.-K., Messer, O. E., Hix, W. R., & Bruenn, S. W. 2001, Phys. Rev. D, 63, 103004
Liebendörfer, M., Rampp, M., Janka, H.-T., & Mezzacappa, A. 2005, ApJ, 620, 840
Lyne, A. G., & Lorimer, D. R. 1994, Nature, 369, 127
MacFadyen, A. I., & Woosley, S. E. 1999, ApJ, 524, 262
MacFadyen, A. I., Woosley, S. E., & Heger, A. 2001, ApJ, 550, 410
Madokoro, H., Shimizu, T., & Motizuki, Y. 2003, ApJ, 592, 1035
Madokoro, H., Shimizu, T. M. & Motizuki, Y. 2004, PASJ, 56, 663
Malesani, D., et al. 2004, ApJ, 609, L5
Matheson, T., et al. 2003, ApJ, 599, 394
Mazzali, P. A., et al. 2005, Science, 308, 1284
Mereghetti, S., Tiengo, A., Israel, G. L. 2002, ApJ, 569, 275
Minkowski, R. 1968, in "Stars and Stellar Systems", 7, 623
Paczynski, B. 1998, ApJ, 494, L45
Pavlov, G. G., & Zavlin, V. E. 1999, IAU Circ. 7270
Pavlov, G. G., Zavlin, V. E., Aschenbach, B., Trümper, J., & Sanwal, D. 2000, ApJ, 531, L53
Pavlov, G. G., Sanwal, D., Garmire, G. P., & Zavlin, V. E. 2002, in Neutron Stars in Supernova Remnants, ed. P. O. Slane & B. M. Gaensler, ASP Conf. Ser. 271 (San Francisco: ASP), 247
Pavlov, G. G., Sanwal, D., & Teter, M. A. 2004, in Young Neutron Stars and Their Environments, IAU Symp. 218, ed. F. Camilo & B. M. Gaensler (San Francisco: ASP), 239
Pavlovsky, C., et al. "ACS Instrument Handbook", Version 5.0, (Baltimore: STScI)
Rampp, M., & Janka, H.-T. 2000, ApJ, 539, L33
Reed, J. E., Hester, J. J., Fabian, A. C., & Winkler, P. F. 1995, ApJ, 440, 706
Reynoso, E. M., & Goss, W. M. 2002, ApJ, 575, 871
Rothschild, R. E. & Lingenfelter, R. E. 2003, ApJ, 582, 257
Scheck, L., Plewa, T., Janka, H.-T., Kifonidis, K., Müller, E. 2004, Physical Review Letters, 92, 011103
Shimizu, T. M., Ebisuzaki, T., Sato, K., & Yamada, S. 2001, ApJ, 552, 756
Stanek, K. Z., et al. 2003, ApJ, 591, L17
Stephenson, F. R., & Green, D. A. 2003, 'The Historical Supernova Remnants', Cambridge University Press, Cambridge UK
Symbalisty, E. M. D. 1984, ApJ, 285, 729
Tananbaum, H. 1999, IAU Circ., 7246
Thompson, C. & Duncan, R. C. 1996, ApJ, 473, 322
Thompson, T. A., Burrows, A., & Pinto, P. A. 2003, ApJ, 592, 434
Thorstensen, J. R., Fesen, R. A., & van den Bergh, S. 2001, AJ, 122, 297
Takiwaki, T., Kotake, K., Nagataki, S., & Sato, K. 2004, ApJ, 616, 1086
Trammell, S. R., Hines, D. C., & Wheeler, J. C. 1993, ApJ, 414, L21
van den Bergh, S. 1971, ApJ, 165, 457
van den Bergh, S., & Dodd, W. W. 1970, ApJ, 162, 485
Walder, R., Burrows, A., Ott, C. D., Livne, E., Lichtenstadt, I., & Jarrah, M. 2005, ApJ, 626, 317
Wang, L., Wheeler, J. C., Li, Z., Clocchiatti, A. 1996, ApJ, 467, 435
Wang, L., Howell, D. A., Höflich, P., & Wheeler, J. C. 2001, ApJ, 550, 1030

Wang, L., et al. 2002, ApJ, 579, 671
Wex, N., Kalogera, V., & Kramer, M. 2000, ApJ, 528, 401
Wheeler, J. C. 2003, Am J. Phys., 71, 11
Wheeler, J. C., Yi, I., Höflich, P., & Wang, L. 2000, ApJ, 537, 810
Wheeler, J. C., Meier, D. L., & Wilson, J. R. 2002, ApJ, 568, 807
Wilson, J. R., Mathews, G. J., & Dalhed, H. E. 2005, ApJ, 628, 335
Winkler, P. F., Roberts, P. F., Kirshner, R. P. 1991, in "Supernovae: The Tenth Santa Cruz Summer Workshop in Astronomy and Astrophysics", ed. S.E. Woosley (Springer-Verlag: New York), p 652
Woosley, S. E. 1993, ApJ, 405, 273
Yamasaki, T., & Yamada, S. 2005, ApJ, 623, 1000

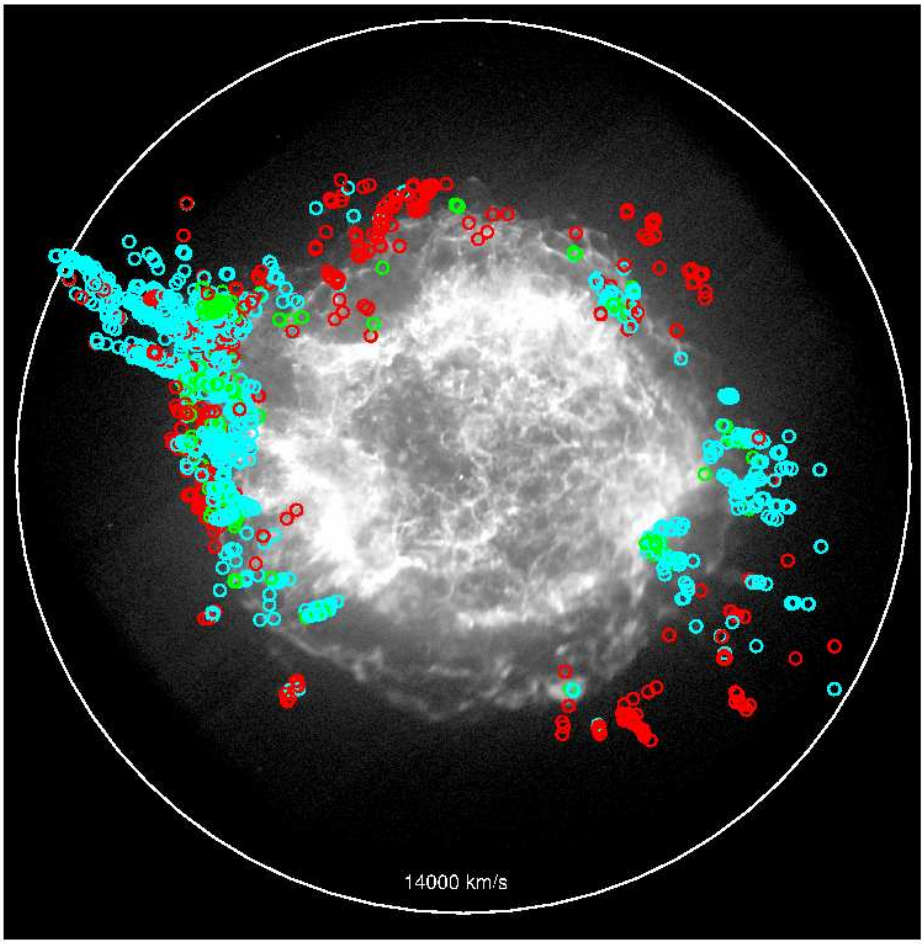


FIG. 1.— The 1 Msec *Chandra* image of Cas A with the locations of the 1825 identified outer ejecta knots (Hammell & Fesen 2006) marked color coded by their emission properties. Red open circles indicate knots with strong [N II] line emission, green open circles knots strong [O II] emission, and blue open circles strong [S II] FMK-like outlying knots.

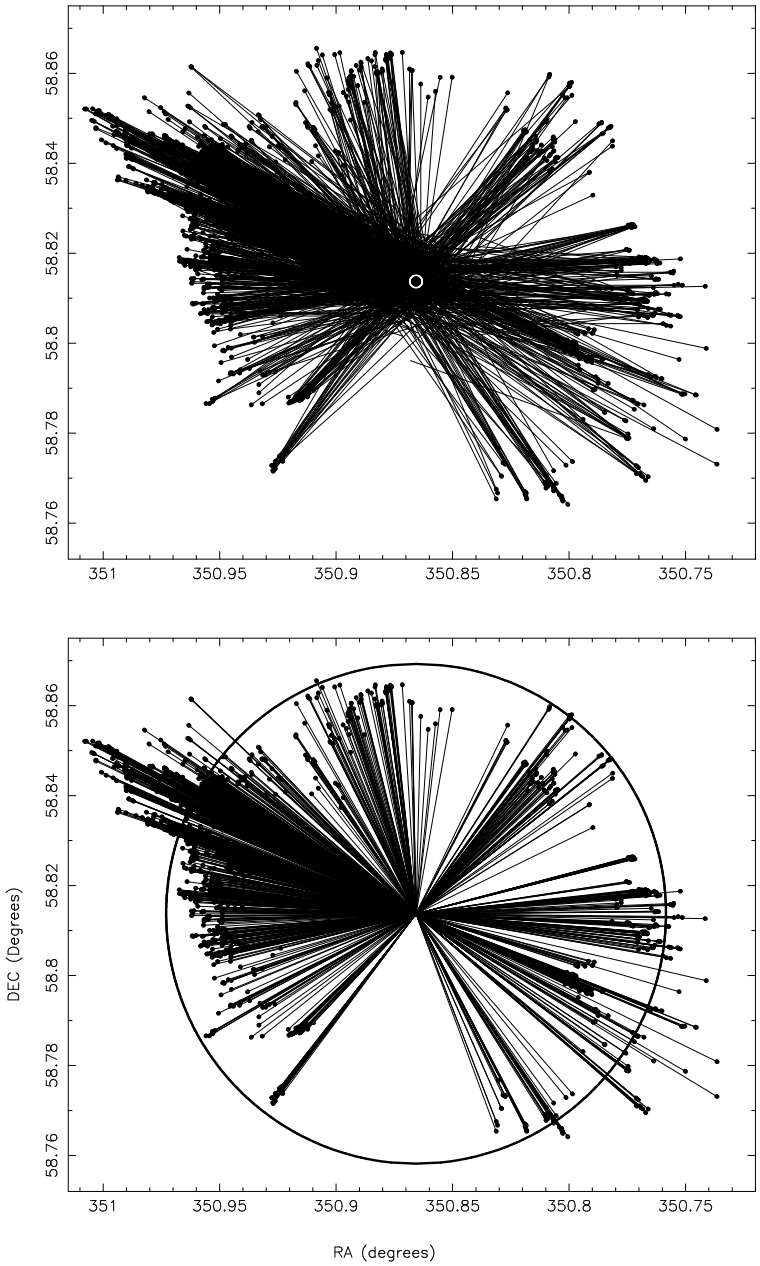


FIG. 2.— *Top:* Plot of extrapolated 320 yr proper motions for the 1825 identified outer knots based on actual proper motions measured using the March and December 2004 ACS/WFC data. Central white circle has a radius of 5″ and marks the remnant's estimated center of expansion (Thorstensen et al. 2001). *Bottom:* Plot of 1825 outer knot positions and their expected motions away from the remnant's known center of expansion revealing a 'bow-tie' asymmetric structure. Circle represents the radial distance of 200″ corresponding to a measured proper motion of 0.″65 $yr^{-1}$ and thus an implied 10,000 km $s^{-1}$ transverse velocity at the assumed remnant distance of 3.4 kpc.

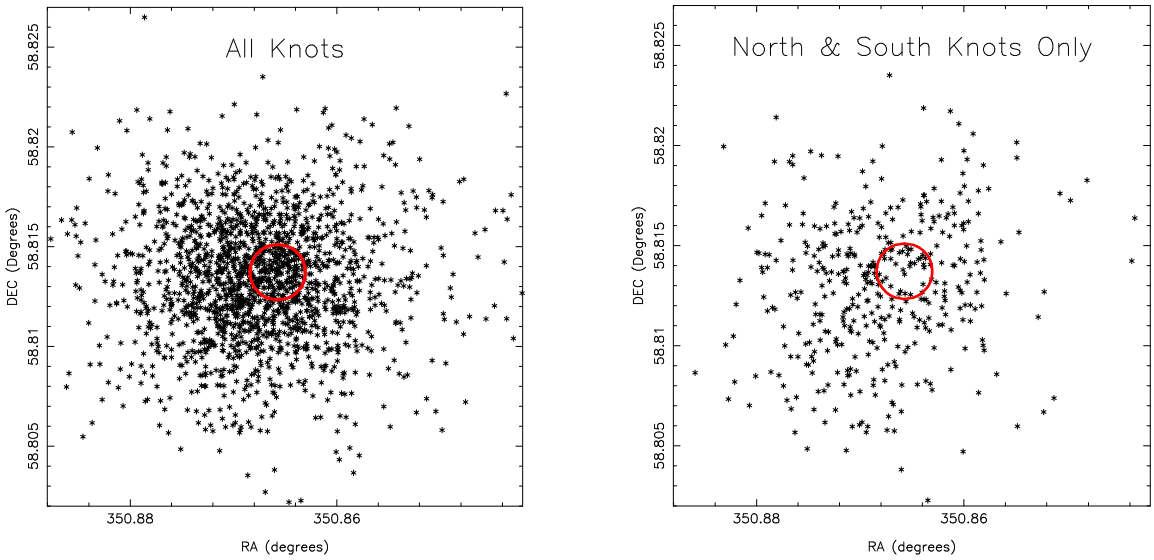


FIG. 3.— *Left Panel:* Plot of extrapolated 1670 epoch positions for 1825 outer ejecta knots relative to the Thorstensen et al. (2001) estimated center of expansion (COE) marked by the grey (red) circle (radius = 5″) centered on $\alpha$(J2000) = $23^{\rm h}23^{\rm m}23^{\rm s}.77$, $\delta = 50°48'49''.4$. The scatter of points is centered 3″.4 from the COE. *Right Panel:* Same as for the left panel except that knots located along the east and west limbs of the remnant have been removed, leaving 416 north and south knots. The scatter of these knots is centered 5″.2 from the COE.

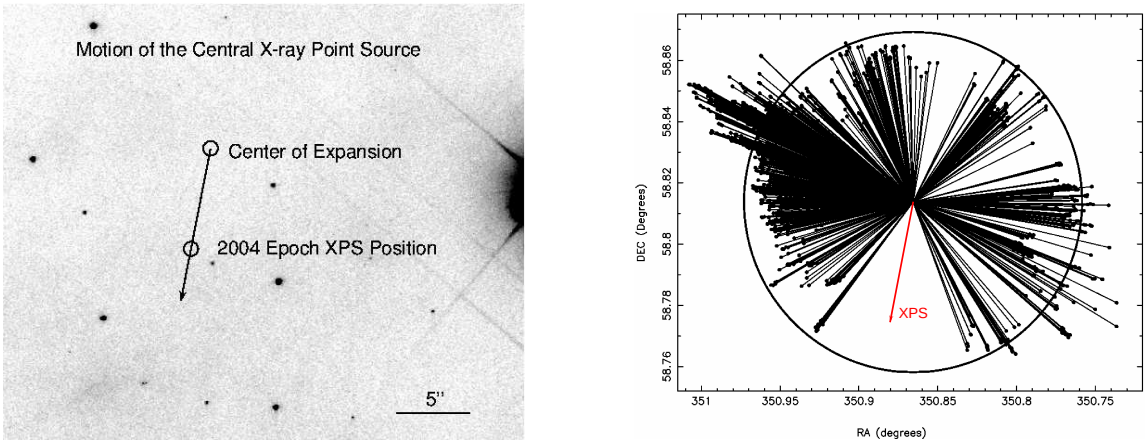


FIG. 4.— *Left Panel:* A 2001 STIS *HST* image of the central region of Cas A near the X-ray Point Source (XPS) with the Thorstensen et al. (2001) expansion center marked ($\alpha[J2000] = 23^{\rm h}23^{\rm m}27^{\rm s}.77 \pm 0^{\rm s}.05$, $\delta[J2000] = 58°48'49''.4 \pm 0''.4$) along with the XPS's current position ($\alpha[J2000] = 23^{\rm h}23^{\rm m}27^{\rm s}.943 \pm 0^{\rm s}.05$, $\delta[J2000] = 58°48'42''.51 \pm 0''.4$) as derived from *Chandra* image data (see Fesen, Pavlov, & Sanwal 2006). The circles marking these positions are 1″ in diameter. The separation between the remnant's estimated expansion center and the XPS' current position is $7''.0 \pm 0''.8$ with an implied motion in a southeasternly direction (position angle = $169° \pm 8.4°$). *Right Panel:* Same plot as shown in the bottom panel of Figure 2 but now showing the apparent motion of Cas A's XPS in the direction of the southern gap of high-velocity, outer ejecta knots.

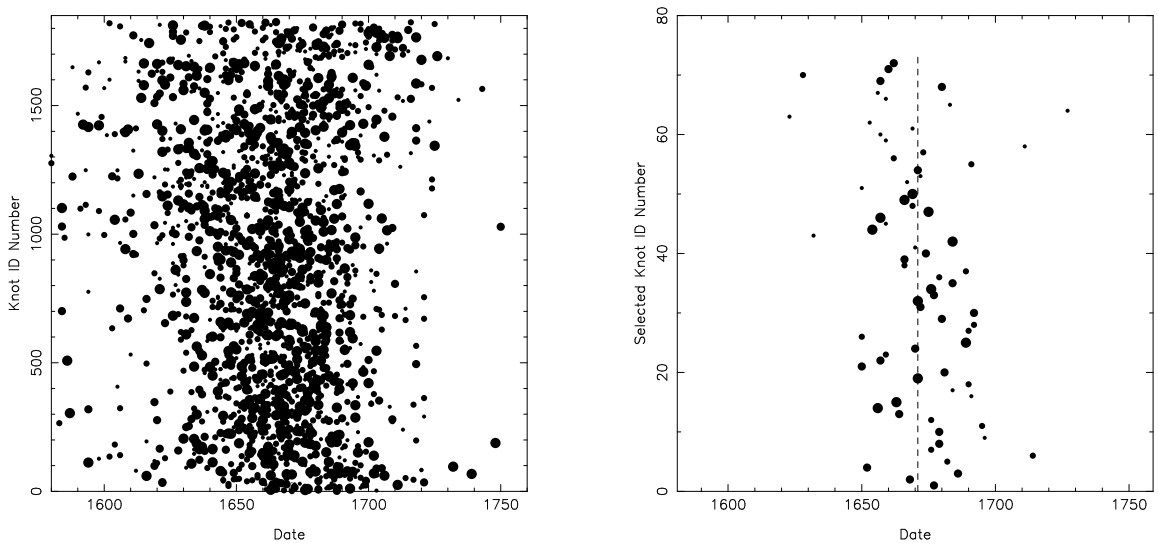


FIG. 5.— *Left Panel:* Plot of catalog knot identification number (ordered in position angle) with the date of closest approach to remnant's estimated center of expansion (COE). Symbol size is inversely proportional to estimated proper motion uncertainty. *Right Panel:* Same as for the left panel but now showing date of closest approach to the COE for 72 selected knots with hand-measured proper motions. Dashed line marks the estimated 1671 convergence date derived by Thorstensen et al. (2001).